Catalysis Letters 34 (1995) 163–177

N_2O decomposition over [Fe]-ZSM-5 and Fe-HZSM-5 zeolites

Y.-F. Chang, J.G. McCarty

Materials Research Center, SRI International, 333 Ravenswood Ave., Menlo Park, CA 94025, USA

and

Y.L. Zhang

Chemistry Department, Fudan University, Shanghai 200433, PR China

Received 31 March 1995; accepted 30 May 1995

The N_2O decomposition over an [Fe]-ZSM-5 and an Fe-HZSM-5 zeolite was studied. We found that framework incorporated iron species were much more active than Fe(III) introduced as framework charge countercations by ion exchange (TOF at 0.1 vol% N_2O: 1.47×10^{-4} at 280°C for [Fe]-ZSM-5 vs. 2.58×10^{-4} at 468°C for Fe-HZSM-5). The higher activity of [Fe]-ZSM-5 was attributed to the uniqueness of framework iron species. Both [Fe]-ZSM-5 and Fe-HZSM-5 zeolites showed enhanced activity in the presence of excess oxygen. This is in sharp contrast to ruthenium exchanged zeolites which showed strong oxygen inhibiting effect on the rate of N_2O decomposition.

Keywords: N_2O (nitrous oxide) catalytic decomposition; [Fe]-ZSM-5 zeolite catalyst; Fe-HZSM-5 catalyst; effect of oxygen on N_2O decomposition rate

1. Introduction

Transition and precious metal cation exchanged ZSM-5 zeolites are reported having high activity for decomposition of nitrous oxide (N_2O) into nitrogen and oxygen [1–8]. Among transition metal cations, Cu^{2+} and Co^{2+} are the most active while Ni^{2+} and Mn^{2+} are the least active in the decomposition of N_2O. Precious metals, Ru, Rh, are superior to transition metals. Previously, we have examined the effect of oxygen on the kinetics of N_2O decomposition over ruthenium exchanged zeolites. It was found that Ru-HNaUSY (ultrastable Y zeolite) is more active than Ru-NaZSM-5 [8]. However, both catalysts exhibited significant decline in activity in the presence of excess oxygen. This limits their practical application as catalysts

for N_2O removal in the presence of excess oxygen and prompts us to investigate other zeolite-based catalysts in order to develop catalysts whose performance may not be strongly inhibited by the presence of excess oxygen. Both iron exchanged and framework incorporated iron zeolites have been examined for N_2O decomposition [1,2,9,10]. For Fe-exchanged Y-zeolite [1] and mordenite [2], the rate data obtained at 350–620°C were represented by rate $= kP_{N_2O}$, where P_{N_2O} is the partial pressure of N_2O; the rate of N_2O decomposition was not inhibited by oxygen. For ferrisilicate analogues (Al-free) of ZSM-5 and ZSM-5 zeolites containing iron in the framework, Panov et al. [4,9,10] found that decomposition of N_2O occurred at temperatures above 150°C. For ferrisilicate ZSM-5, the N_2O decomposition was divided into two regions [10]. In the low temperature region ($\leqslant 300$°C), the reaction was predominated by decomposing N_2O to dinitrogen as a gas phase product and atomic oxygen retained by the catalyst. In the high temperature region (>300°C), the reaction was complete, leading to the formation of stoichiometric amounts of gas phase N_2 and O_2. The above results were obtained in a static vacuum (10^{-6}–10^{-7} Torr) system.

In the present study, in order to find zeolite based catalysts which are highly active at low temperatures (<400°C) and whose activities are not inhibited by oxygen we investigated the effect of oxygen on the kinetics of N_2O decomposition over a framework-iron containing [Fe]-ZSM-5 and an Fe^{3+}-exchanged Fe-HZSM-5 zeolite catalyst under flow conditions. We found that [Fe]-ZSM-5 was highly active for N_2O decomposition at temperatures >200°C, while Fe-HZSM-5 required temperature above 400°C. More importantly, both catalysts showed positive oxygen dependence in N_2O decomposition rate. Therefore, [Fe]-ZSM-5 is a potential catalyst for N_2O decomposition, especially in the presence of oxygen.

2. Experimental

2.1. CATALYST PREPARATION

2.1.1. [Fe]-ZSM-5

[Fe]-ZSM-5, the iron(III) isomorph of aluminosilicate ZSM-5, was prepared by a method similar to that described previously [11–13]. Typically, the procedure involved the mixing of three solutions: solution A contained sodium silicate made from water glass, mixed with sodium hydroxide and water; solution B contained *n*-butylamine dissolved in water and solution C contained hydrated iron(III) nitrate dissolved in a sulfuric acid solution. After mixing the solutions in the above order, the resulting gel was heated to 160°C in a 500 cm^3 stainless-steel autoclave with continuous stirring (300 RPM). The crystallization process took approximately 72 h. During this process an acid perturbation was applied after 20 h heating at 160°C to assist the development of crystallites.

After crystallization, the products were filtered off, dried at 110°C for 2 h and calcined at 550°C for 6 h. The composition of the zeolite prepared determined by atomic absorption and ion exchange is given in table 1.

2.1.2. Fe-HZSM-5

Fe-HZSM-5 was prepared by exhaustive exchange of H-ZSM-5 ($[H^+] = 0.56$ mmol g^{-1}) with 1.0 M $Fe(NO_3)_3$ aqueous solution at room temperature. The amount of Fe(III) exchanged into the zeolite was determined by titrating the proton replaced by Fe^{3+}. The composition of Fe-HZSM-5 is also presented in table 1.

2.2. CATALYTIC ACTIVITY MEASUREMENTS

The catalytic decomposition of N_2O over [Fe]-ZSM-5 and Fe-HZSM-5 zeolite catalysts was conducted in a flow micro-reactor. The tubular reactor (i.d.: 3.5 mm) was quartz and contained a fused quartz frit to hold the catalyst sample. 100 mg of catalyst was used for each run. A quartz sheathed thermocouple touched the catalyst bed from the top. The catalyst was first treated in flowing (20 cm^3 min^{-1}) 10 vol% oxygen during heating from 40 to 700°C at a heating rate of 30°C min^{-1}, held at 700°C for 30 min, then cooled to 40°C at 30°C min^{-1} in the same gas stream. Temperature programmed reaction (TPR) was used for kinetic measurements. Prior to the TPR the catalyst was purged in high purity helium (40 cm^3 min^{-1}) at 40°C for 30 min and was then treated at the same temperature in the reaction stream for 10 min. The total flow rate of the feed gases used was 40 cm^3 min^{-1}. Two gas mixtures and a high purity helium were used, 1 vol% N_2O in helium (Liquid Carbonic), 10 vol% O_2 with 1 vol% Ar (as a mass spectrometry tracer) in helium (Liquid Carbonic), and high purity helium (99.999%, Liquid Carbonic). During the rate measurements, the concentration of N_2O varied in the range 0.05–0.5 vol% and oxygen in the range 0–5 vol%, thus giving O_2/N_2O ratios ranging from 0 to 100. Product gas concentrations in the reaction effluents were analyzed by an on-line quadrupole mass spectrometer (Electronic Associates, Inc.), using AMU 2 for hydrogen, 32 for oxygen, 40 for argon, 46 for nitrogen dioxide, 28 for nitrogen, and 44 for nitrous oxide.

Table 1
Composition and some properties of [Fe]-ZSM-5 and Fe-HZSM-5

Catalyst	Fe (wt%)	Al (wt%)	Number of Fe^{3+} (μmol g^{-1})	Number of protons (μmol g^{-1}) [b]
[Fe]-ZSM-5	2.80	0.53	525 [b]	0
Fe-HZSM-5	0.56 (59%) [a]	1.52	110	230

[a] Value in parentheses is the degree of Fe^{3+}-exchange based on the assumption that each Fe^{3+} replaces three protons.

[b] All iron present are assumed to be in the framework.

3. Results and discussion

3.1. DECOMPOSITION OF N_2O OVER [Fe]-ZSM-5

Temperature programmed reaction (TPR) experiments of N_2O in the absence of oxygen and in the presence of different levels of oxygen (0.25–5.0 vol%) were conducted over [Fe]-ZSM-5. As two examples, the TPR profiles of 0.1 vol% N_2O and 0.25 vol% N_2O over [Fe]-ZSM-5 are given in figs. 1a and 1b, respectively. In the low temperature region (<200°C), desorption of N_2O occurred but no significant N_2O decomposition took place. Fig. 1a shows that the N_2O decomposition occurred at temperatures above 240°C. Fig. 2 presents the TPR of 0.1 vol% N_2O in the presence of different levels of oxygen at temperatures above 200°C. The pres-

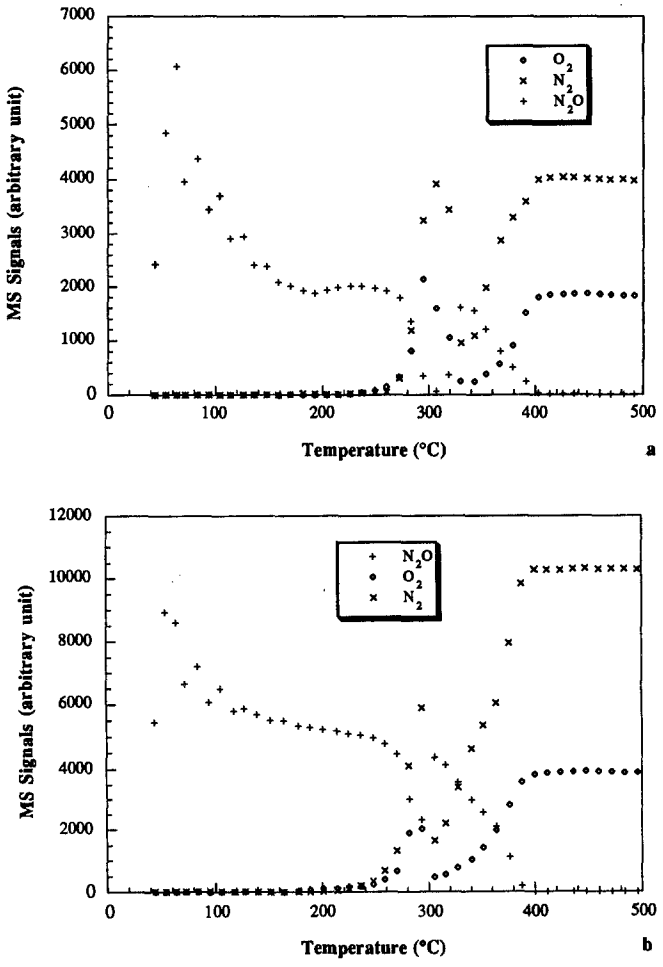

Fig. 1. TPR profiles of 0.1 vol% N_2O and 0.25 vol% N_2O over [Fe]-ZSM-5 (catalyst: 0.1 g; total flow rate: 40 cm^3 min^{-1}; ramp rate: 30°C min^{-1}).

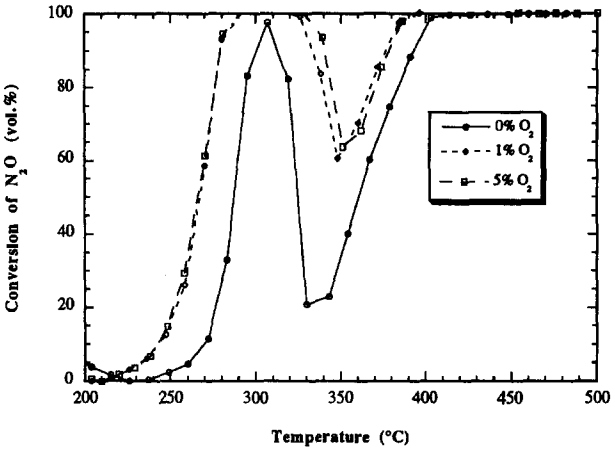

Fig. 2. TPR profiles of 0.1 vol% N_2O over [Fe]-ZSM-5 at different levels of oxygen (catalyst: 0.1 g; total flow rate: 40 cm^3 min^{-1}; ramp rate: 30°C min^{-1}).

ence of oxygen (1–5 vol%) led to lowering the temperature required for N_2O decomposition from 240°C in the absence of oxygen to 210°C. Declining of activity occurred at 310–400°C. The decline was far more pronounced in the absence of oxygen than in the presence of 1–5 vol% oxygen. Since the catalysts had been treated in 10 vol% oxygen at 700°C for 30 min before the N_2O TPR experiments were conducted, we believe that both framework and non-framework iron species were in the high oxidation state, i.e., Fe^{3+}. This was confirmed by subsequent TPO in 10 vol% oxygen. No consumption of oxygen occurred during the treatment from 40 to 700°C, suggesting there was neither oxidation of the catalyst nor oxygen uptake by the catalyst.

The transient activity (the decline of activity between 310 and 400°C during TPR) observed in the present work was not observed by Panov et al. [4,9,10]. If the activity measurement (N_2O conversion) is solely based on detection of N_2O in the effluent without monitoring the products (N_2, O_2, and others), then desorption of N_2O could be misinterpreted as decline of activity. However, in our experiments, we monitored all the possible products. As shown in figs. 1a and 1b, the increase of N_2O in the effluent is accompanied by simultaneous and proportional decline of products N_2 and O_2. Therefore, the transient activity is not an artifact. However, we do not understand the cause for it.

Due to the low iron contents (Fe: <1 wt%) of the samples used by Panov et al. [4,9,10], presumably, all the iron is in the framework, in other words, the amount of non-framework iron is negligible. Thus, the transient activity observed in the present study may relate to the presence of non-framework iron. Nevertheless, the high activity at low temperature is not fully due to the presence of non-framework iron because Panov et al. demonstrated that ferrisilicates free of non-framework iron also showed high low-temperature activity [9,10].

Mössbauer spectroscopy has shown that the iron ions in ferrisilicate are tetrahedrally coordinated Fe^{3+} [14,15] and that those in iron oxide supported on silicalite, isostructural to ZSM-5 but containing no aluminium in the framework, or silica are octahedrally coordinated Fe^{3+} in the form of small particles of α-Fe_2O_3 [15,16]. It is concluded [15] that the activity (per Fe site) of tetrahedrally coordinated Fe^{3+} in ferrisilicate framework for CO oxidation by oxygen was much lower (by one order of magnitude) than that of the octahedrally coordinated Fe^{3+} in the iron-oxide-impregnated silicalite or the Fe cations in the Fe-ZSM-5 prepared by an ion-exchange method.

We noticed very slight coloring of [Fe]-ZSM-5 catalyst after temperature programmed oxidation in 10 vol% oxygen and subsequent N_2O TPR measurements. It changed from white to light brownish. The brownish color is an indication of formation of extra-framework Fe^{3+} species. Others also found a slight color change to off-white when an [Fe]-ZSM-5 sample was calcined at 500°C in air [14] and a light brown coloration of [Fe]-β zeolite when it was calcined at temperature exceeding 500°C [17]. However, X-ray diffraction measurements conducted on our [Fe]-ZSM-5 zeolite samples which were treated in 10 vol% oxygen at 700°C for 30 min and used for N_2O TPR at up to 700°C showed no bulk Fe_2O_3, suggesting that either the amount of extraframework iron species formed is not significant or the iron species are highly dispersed as small iron oxide clusters which cannot be detected by XRD. The lack of bulk Fe_2O_3 phase in [Fe]-ZSM-5 even after severe treatments is consistent with our surface area measurement results, where a BET surface area of 300 m^2/g was obtained for [Fe]-ZSM-5. This value is similar to that of Fe-HZSM-5 (BET: 290 m^2/g) and lower than that reported by Inui et al. [18] for ferrisilicate ZSM-5 (BET: $\sim$ 350 m^2/g). The high BET surface area is in consistence with the high Fe dispersion in the zeolite crystal.

3.2. H_2-TPRd AND CO-TPD

To investigate whether non-framework iron species are present in [Fe]-ZSM-5 zeolite and the stability of framework iron species under different reduction and oxidation treatment conditions, temperature programmed hydrogen reduction (H_2-TPRd), temperature programmed oxidation (TPO), CO-TPD were conducted. H_2-TPR and CO-TPD spectra are presented in figs. 3 and 4, respectively.

The H_2-TPRd spectrum shows three major reduction peaks at 368, 400, and 415°C. The reduction took place at temperatures above 300°C and was complete at about 440°C. The amount of hydrogen consumed during the TPRd is 105 $\mu mol\ g^{-1}$.

The overall reduction stoichiometry of transition metal ions as charge-compensating cations in X, Y, and MOR zeolites [19,20] is well documented. For most transition metal cations, a reduction temperature above 350°C is required [21–23]. Depending on whether water is generated during the reduction, the location of the cation can be determined. For charge-compensating cations, their reduction does

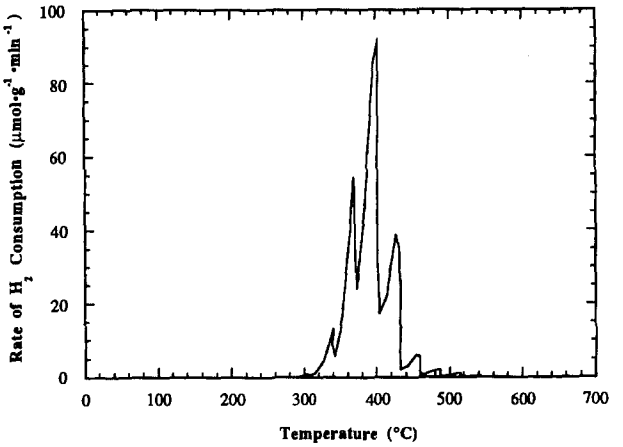

Fig. 3. TPRd of [Fe]-ZSM-5 in 1.9 vol% hydrogen (catalyst: 0.1 g; total flow rate: 40 cm^3 min^{-1}; ramp rate: 30°C min^{-1}).

not produce water because of formation of protonium ions which compensate the framework charge (reaction (1)). On the other hand, if cations are not at charge-compensating positions their reduction leads to formation of water according to reaction (2):

$$M^{n+} + \tfrac{1}{2}nH_2 \rightarrow M + nH^+ \quad (1)$$

$$MO_x + xH_2 \rightarrow M + xH_2O\,, \quad (2)$$

where M represents transition metal. Thus, the formation of water is a clear indication of the presence of bulk metal oxides or non-framework species not located at

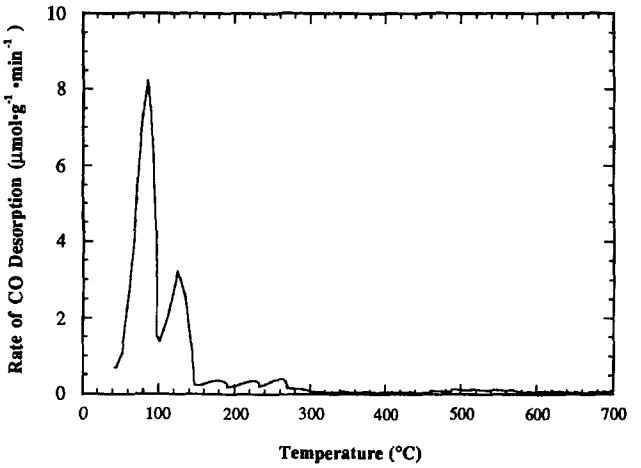

Fig. 4. TPD of CO adsorbed on [Fe]-ZSM-5 at 40°C (catalyst: 0.1 g; total flow rate: 40 cm^3 min^{-1}; ramp rate: 30°C min^{-1}).

charge-compensating positions. Our XRD results on the fresh [Fe]-ZSM-5, used [Fe]-ZSM-5 in TPO, H_2-TPRd, CO-TPRd, and CO-TPD experiments, and used [Fe]-ZSM-5 in N_2O-TPR experiments do not reveal any significant changes in the crystallinity, suggesting that neither reduction/oxidation treatment nor N_2O-TPR causes any changes in the ZSM-5 crystal structure. BET measurements of the above three catalyst samples show no significant changes in total surface area, suggesting the integrity of the crystal structure and the absence of pore plugging or blocking by non-framework species. This suggests that the species reduced by hydrogen treatment are those which are not located in the framework positions and that they are highly dispersed so that no pore blockage or plugging occurs. We noticed that during H_2-TPRd the consumption of hydrogen was accompanied by the formation of water. Judging from the amount of water formed the majority of the iron species reduced are located in the non-framework and non-charge-compensating positions. This is in agreement with previous findings that framework charge-compensating Fe^{3+} can only be reduced to Fe^{2+} in hydrogen, only non-framework bulk iron oxides could be reduced to the metallic state [24–26]. Based on the amount of hydrogen consumed and assuming that all hydrogen was used for reduction of Fe_2O_3 to metallic iron species, we estimated that the amount of reducible iron species is 71 $\mu mol\ g^{-1}$, which corresponds to approximately 14% of total iron in the zeolite. However, this is not conclusive about whether they are formed during the calcination/oxidation/reduction treatments or present in the as-synthesized sample.

Framework Fe^{3+} in ferrisilicate, for example, [Fe]-ZSM-5, are very stable. Using ESR, Ione et al. [27] showed that [Fe]-ZSM-5 gives signals with g factors of 4.3 associated with framework Fe^{3+} (tetrahedral coordination), as well as signals with g factors of 2.3 and 2.0 usually associated with non-framework Fe^{3+} (octahedral coordination). Upon reduction at 600°C in hydrogen, only the ESR signal with $g = 2.0$ disappears. Upon washing with 1.0 M hydrochloric acid solution, the two signals at $g = 2.0$ and $g = 2.3$ vanish. Using fluorescence spectroscopy, Krustov et al. [28] found that the characteristic four band spectrum of framework Fe^{3+} is not affected by reduction in carbon monoxide or hydrogen at temperatures 400–800°C. These results strongly indicate that framework Fe^{3+} are very stable against reduction of acid treatment.

However, using ESR, Kaliaguine et al. [29] found that a new signal at $g = 5.3$ appeared when the ferrisilicate sample was calcined at 520°C in air. The signal at $g = 5.3$ was attributed to highly distorted tetrahedrally coordinated Fe^{3+}. The fact that signals at $g = 5.3$ and $g = 2.0$ increased in intensity while the one at $g = 4.3$ was reduced, suggests that some Fe^{3+} ions are removed from their framework position forming occluded iron oxide. Therefore, although framework Fe^{3+} are very stable under reducing conditions, removal of irons from their framework position can occur upon calcination at high temperatures.

Recently, the influence of treatments such as calcination in air, evacuation, and reduction in hydrogen at different temperatures on the stability of lattice Fe^{3+}

ions of β-zeolite has been studied by Raj et al. [30]. Szostak et al. [31] found that Fe^{3+} ions in zeolite framework are less stable than Al^{3+} ions. At high temperatures, especially in the presence of steam, they tend to leave the framework position and form bulk iron oxide species either inside the zeolites channels or on the external surface depending on the severity of the treatment. In addition, auto-reduction to Fe^{2+} may also occur, leaving the framework position [32]. After having left the framework positions these iron species can either occupy charge-compensating positions or become non-framework species. In the latter case, these species will be oxidized, migrate, and sinter to form bulk oxide.

To confirm that the catalytic activity observed is caused by the framework iron species and not by the non-framework iron species we conducted N_2O-TPR on an [Fe]-ZSM-5 zeolite sample whose non-framework irons supposedly had been removed according to a procedure previously described [12]. The [Fe]-ZSM-5 was refluxed with a solution containing hydroxyamine chloride (0.2 M) and sodium citrate (0.03 M). The N_2O-TPR results obtained on the treated [Fe]-ZSM-5 sample are identical to the untreated [Fe]-ZSM-5. Therefore, we conclude that it is the framework Fe^{3+} species of [Fe]-ZSM-5 zeolite which are responsible for the low-temperature (250–300°C) activity for N_2O decomposition. Though extra-framework iron species were formed after treatments at high temperatures (up to 700°C) they are not responsible for the low-temperature activity.

3.3. CO-TPD

A TPD followed CO adsorption at 40°C shows two CO desorption peaks at 85 and 115°C. The amount of CO adsorbed at 40°C estimated from the TPD experiment is 8 μmol g^{-1}. This represents a very small fraction of the total amount of irons present in the zeolite. Therefore, the sites which are responsible for the CO desorption peaks are not framework irons, otherwise we would expect a much higher level of CO uptake. It is likely that the CO desorption peaks are related to non-framework iron species. More work is required to clarify the sites responsible for CO adsorption.

3.4. DECOMPOSITION OF N_2O OVER Fe-HZSM-5

The TPR profiles of N_2O decomposition in the absence of oxygen and in the presence of different levels of oxygen (0.25–5 vol%) over Fe^{3+}-exchanged H-ZSM-5 are presented in fig. 5. Similar to that of [Fe]-ZSM-5, in the low temperature region (<300°C), desorption of N_2O occurred but no significant N_2O decomposition took place. Fig. 2 shows that significant N_2O decomposition occurred at temperatures above 400°C. The presence of oxygen (1–5 vol%) led to lowering the temperature required for N_2O decomposition from 450°C in the absence of oxygen to 350°C. The decline of activity which occurred at 310–400°C observed for [Fe]-ZSM-5 was not observed for Fe-HZSM-5.

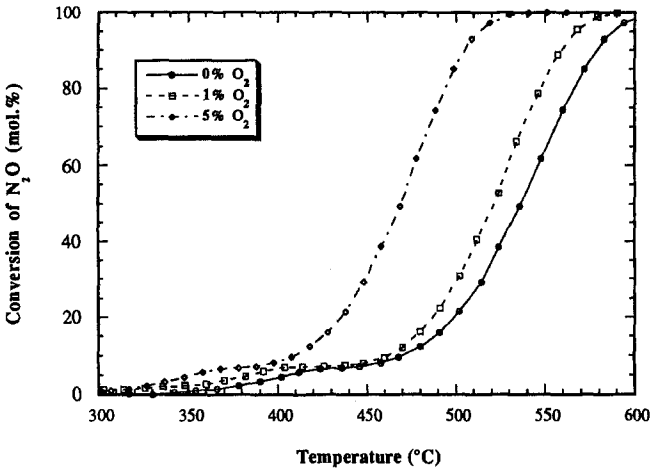

Fig. 5. TPR profiles of 0.1 vol% N_2O over Fe-HZSM-5 at different levels of oxygen (catalyst: 0.1 g; total flow rate: 40 cm^3 min^{-1}; ramp rate: 30°C min^{-1}).

The TPR results obtained at various N_2O concentrations on both [Fe]-ZSM-5 and Fe-HZSM-5 catalysts in the presence of different levels of oxygen are given in table 2. They show that for both catalysts, higher N_2O partial pressures result in greater turnover frequencies and that the presence of oxygen enhances the TOF.

Table 2
Comparison of the activities of [Fe]-ZSM-5 and Fe-HZSM-5 zeolite catalysts for N_2O decomposition

Catalyst	Temperature (°C)	N_2O conc. (vol%)	O_2 conc. (vol%)	TOF (molec. of N_2O Fe^{-1} s^{-1})
[Fe]-ZSM-5	270	0.05	0	0.09×10^{-4}
	280	0.05	0	0.15×10^{-4}
	270	0.1	0	0.49×10^{-4}
	280	0.1	0	1.47×10^{-4}
	270	0.25	0	1.91×10^{-4}
	280	0.25	0	5.02×10^{-4}
	270	0.375	0	6.34×10^{-4}
	280	0.375	0	12.80×10^{-4}
	270	0.1	0.25	2.60×10^{-4}
	270	0.1	1	2.95×10^{-4}
	270	0.1	5	3.30×10^{-4}
Fe-HZSM-5	468	0.1	0	2.58×10^{-4}
	465	0.25	0	6.81×10^{-4}
	468	0.375	0	9.74×10^{-4}
	470	0.1	0.25	3.65×10^{-4}
	470	0.1	1	4.58×10^{-4}
	470	0.1	5	10.72×10^{-4}

The kinetics data derived from TPR results obtained at N_2O conversion below 30% as a power law rate expression, $-dN_2O/dt = k(P_{N_2O})^m(P_{O_2})^n$ (where P_{N_2O} and P_{O_2} represent the partial pressure of N_2O and O_2 respectively), are presented in table 3.

As an example, the dependence of N_2O decomposition rate on N_2O partial pressure in the absence of oxygen over [Fe]-ZSM-5 catalyst at 270°C is given in fig. 6. The N_2O decomposition rate shows a second-order dependence on N_2O partial pressure. This N_2O dependence varies slightly with temperature.

The effect of oxygen partial pressure on N_2O decomposition rate over [Fe]-ZSM-5 catalyst is given in fig. 7. The N_2O decomposition rate has a moderate positive-order oxygen partial pressure dependency. The order of oxygen-dependency varies slightly with temperature.

The apparent activation energy of Fe-HZSM-5 in N_2O decomposition in the absence of oxygen (200 kJ mol^{-1}) is much higher than that of Fe-HZSM-5 (120 kJ mol^{-1}). The apparent activation energy observed for [Fe]-ZSM-5 in the absence of oxygen is very close to those reported for Fe^{3+}-Y [1] and Fe^{3+}-mordenite [2] zeolites (130–140 kJ mol^{-1}) and for ferrisilicate [10] (110–140 kJ mol^{-1}). The data of table 3 show that, for [Fe]-ZSM-5 zeolite, the presence of oxygen results in higher activity and lower apparent activation energy (from $\sim$ 200 kJ mol^{-1} to $\sim$ 140 kJ mol^{-1}). For Fe-HZSM-5 zeolite, the presence of excess oxygen ($\geq$1 vol%) also leads to lower apparent activation energy (from 120 kJ mol^{-1} to $<$100 kJ mol^{-1}). For [Fe]-ZSM-5 catalyst the reaction rate is second order with respect to N_2O, but Fe-HZSM-5 has a first-order dependence on N_2O partial pressure. Both catalysts show similar moderate positive reaction orders with respect to oxygen partial pressure. This suggests that the recombination of atomic oxygen formed from direct decomposition of N_2O to form gas phase oxygen is not a rate-limiting step. Otherwise, a negative-order oxygen dependency should have been observed. The present result supports previous findings reported for Fe^{3+}-mordenite and Fe^{3+}-Y zeolites [1,2] where zero-order oxygen dependence was observed.

The moderate positive-order oxygen partial pressure dependency in N_2O decomposition over both [Fe]-ZSM-5 and Fe-HZSM-5 zeolite catalysts observed in the

Table 3
Comparison of power law kinetic results of N_2O decomposition based on $-dN_2O/dt = k(P_{N_2O})^m(P_{O_2})^n$

Catalyst	Reaction order to N_2O m	Reaction order to O_2 n	Apparent activation energy E_a (kJ mol^{-1}) [a]
[Fe]-ZSM-5	2.0 ± 0.05	0.15 ± 0.05	220 ± 20 (130 ± 15) [b]
Fe-HZSM-5	1.0 ± 0.05	0.35 ± 0.10	140 ± 20 (100 ± 30) [c]

[a] Number in parentheses obtained in the presence of oxygen (0.25–5 vol%).
[b] E_a: estimated in the temperature range of 200–280°C.
[c] E_a: estimated in the temperature range of 420–550°C.

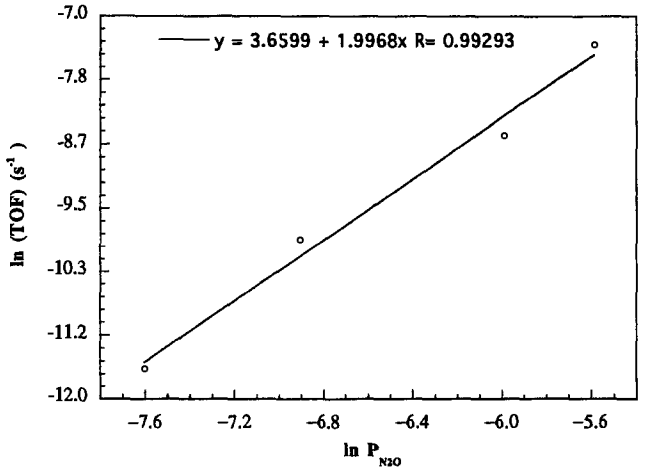

Fig. 6. Dependence of N_2O decomposition rate on N_2O partial pressure over [Fe]-ZSM-5 at 270°C.

present study is consistent with the results for Fe(III)-Y reported by Fu and coworkers [1] and for Fe(III)-mordenite reported by Leglise and coworkers [2], where the decomposition of N_2O was not inhibited by oxygen. Our results are in contrast to the results obtained for metal oxides and perovskites [33–35] where oxygen has a strong inhibition effect on N_2O decomposition rate and to Ru-exchanged ultrastable Y [8] and Na-ZSM-5 zeolites [6,36].

The positive-order oxygen partial pressure dependency of [Fe]-ZSM-5 and Fe-HZSM-5 may relate to their high activity for isotope exchange between gas phase oxygen and zeolite lattice oxygen. Previous work by Panov et al. [4,37] and Uddin et al. [17] on isothermal oxygen isotope exchange of ferrisilicate ZSM-5, and

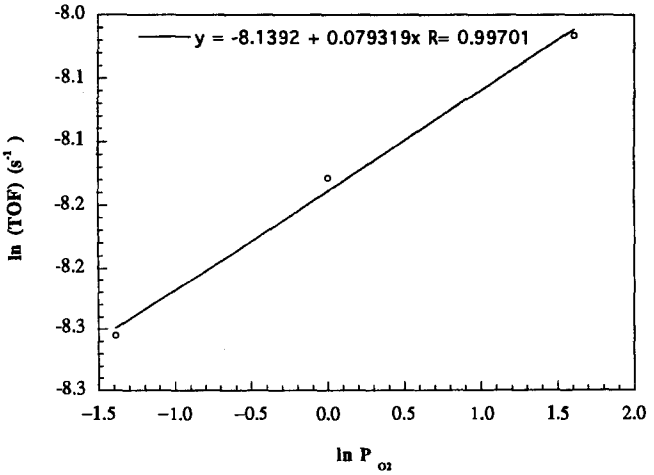

Fig. 7. Dependence of N_2O decomposition rate on O_2 partial pressure over [Fe]-ZSM-5 at 270°C.

Chang et al. [38] on temperature programmed oxygen isotope exchange of Fe-HZSM-5 zeolite showed that both framework iron species and iron cations introduced by ion exchange show substantial activity for isotope oxygen exchange between gas phase oxygen and zeolite framework oxygen at temperatures $\geqslant 300°C$. The high mobility of surface oxygen of both [Fe]-ZSM-5 and Fe-HZSM-5 indicates that the oxygen is not strongly bonded to the iron species. Consequently, desorption of oxygen to form gas phase oxygen will not be a rate-limiting step in N_2O decomposition.

The sharp contrast between [Fe]-ZSM-5 which shows very high activity for N_2O decomposition at temperatures 250–300°C and Fe-HZSM-5 which is not active until temperatures above 400°C strongly suggests that the low-temperature activity is not caused by framework charge countercation Fe^{3+} species. However, one cannot rule out possible contribution from extra-framework iron species (neither framework irons nor framework charge countercation irons). Using Mössbauer spectroscopy, Raj et al. [30] found that upon calcination of [Fe]-β zeolite at temperatures around 450°C some framework Fe^{3+} (tetrahedrally coordinated) transformed into Fe^{3+} (octahedrally coordinated), suggesting that high temperature calcination results in losing framework iron. At higher temperatures ($>500°C$) the transformation of framework iron to non-framework iron species is more significant. However, there is also evidence [30,39] indicating that the iron species removed from the framework can revert back to the framework when treated under reducing conditions or re-calcined at less severe conditions, and non-framework iron species are incorporated into zeolite framework at temperatures above 300°C [40,41]. For Fe-HZSM-5 catalyst, we did not notice (see fig. 5) any significant increase in the low-temperature activity caused by framework Fe^{3+} even after up to 40 cycles of ramp-up and ramp-down, suggesting that there was no reverting of framework charge balancing Fe^{3+} into framework or the amount of Fe^{3+} incorporated is too low to be detected by our TPR experiments. Thus, for Fe-HZSM-5, its activity is solely due to Fe^{3+} present as framework charge-compensating cations.

The reason that in Fe-HZSM-5 no incorporation of non-framework iron into framework occurs is that all the Fe^{3+} ions occupy the charge-compensating positions, in other words, are in cationic positions. The incorporation of cations into framework requires other cations to compensate the charge created by incorporation of the cations and the charge deficit because of conversion of the non-framework cations into framework cations. In the case of Fe-HZSM-5, it is impossible for the cationic Fe^{3+} to meet the two needs. Thus, direct incorporation of charge-compensating Fe^{3+} into zeolite framework did not occur. However, this may be possible in cases where Fe^{2+} are charge-compensating cations. Oxidation of Fe^{2+} to Fe^{3+} can compensate the charges created by incorporation of Fe^{3+} into the zeolite framework.

Another possibility is where protons are generated. The lack of both framework Fe^{3+} and non-framework iron ions in Fe-HZSM-5 compared with [Fe]-ZSM-5

leads us to believe that the decline in catalytic activity of [Fe]-ZSM-5 zeolite in N_2O decomposition must be associated with Fe^{3+} removal from the framework or re-incorporating of non-framework Fe^{3+} into framework. Based on the temperature where decline of activity occurs, the temperature is probably too low to cause removal of Fe^{3+} from the framework. Normally, removal of framework Fe^{3+} requires temperatures above 500°C. Thus, the decline of activity can only be attributed to changes associated with non-framework iron species. Complete incorporation of non-framework iron into framework position can be ruled out because formation of the latter should lead to higher N_2O decomposition rate. The influence of non-framework iron species on the behavior of [Fe]-ZSM-5 catalyst in N_2O decomposition reaction deserves further investigation. It seems that the presence of oxygen reduces the influence of non-framework iron species.

4. Conclusions

An [Fe]-ZSM-5 zeolite prepared by direct synthesis was found highly active for N_2O decomposition at low temperatures (250–300°C). Rate measurements using TPR technique revealed that decomposition of N_2O over [Fe]-ZSM-5 was second order in N_2O partial pressure and had moderate positive power law dependence on oxygen partial pressure. The low-temperature activity exhibited by [Fe]-ZSM-5 is due to its framework irons which are not present in Fe-HZSM-5. The significant decline in activity occurring at >300°C, especially in the absence of oxygen or at low oxygen concentration, may be caused by changes of non-framework iron species. In contrast to [Fe]-ZSM-5, Fe-HZSM-5 is only active at temperatures above 400°C. Its kinetic rate data are described by a first-order dependence on N_2O partial pressure and a moderately positive oxygen partial pressure dependence.

References

[1] C.M. Fu, V.N. Korchak and W.K. Hall, J. Catal. 68 (1981) 166.
[2] J. Leglise, J.O. Petunchi and W.K. Hall, J. Catal. 86 (1984) 392.
[3] L.M. Aparicio, M.A. Ulla, W.S. Milman and J.A. Dumesic, J. Catal. 110 (1988) 330.
[4] G.I. Panov, V.I. Sobolev and S. Kharitonov, J. Mol. Catal. 61 (1990) 85.
[5] M. Tabata, H. Hamada, Y. Kindachi, M. Sasaki and T. Ito, Chem. Exp. 7 (1992) 77.
[6] Y.-J. Li and J.N. Armor, Appl. Catal. B 1 (1992) L21-29.
[7] Y.-J. Li and J.N. Armor, US Patent 5171553 (1992).
[8] Y.-F. Chang, J.G. McCarty, E.D. Wachsman and V. Wong, Appl. Catal. B 84 (1994) 283.
[9] V.I. Sobolev, O.N. Kovalenko, A.S. Kharitonov, Y.D. Pankratiev and G.I. Panov, Mendeev's Commun. 1 (1991) 29.
[10] V.I. Sobolev, G.I. Panov, A.S. Kharitonov, V.N. Romannikov, A.M. Volodin and K.G. Ione, J. Catal. 139 (1993) 435.
[11] R. Szostak and T.L. Thomas, J. Catal. 100 (1986) 555.
[12] G.P. Handreck and T.D. Smith, J. Chem. Soc. Faraday Trans. I 85 (1989) 3195.

[13] Y.-L. Zhang, PhD Thesis, Fudan University, PR China (1994).
[14] A. Meagher, V. Nair and R. Szostak, Zeolites 8 (1988) 3.
[15] M.A. Uddin, T. Komatsu and T. Yoshima, Microporous Mater. 1 (1993) 201.
[16] J. Galuszka, T. Sato and J.K. Sawacki, J. Catal. 136 (1992) 96.
[17] M.A. Uddin, T. Komatsu and T. Yoshima, J. Catal. 146 (1994) 468.
[18] T. Inui, H. Matsuda, O. Yamase, H. Nagata, K. Fukuda, T. Ukawa and A. Miyamota, J. Catal. 98 (1986) 491.
[19] P.A. Jacobs, *Carboniogenic Activity of Zeolites* (Elsevier, Amsterdam, 1977).
[20] O.D. Delafosse, in: *Catalysis by Zeolites*, eds. B. Imelik et al. (Elsevier, Amsterdam, 1980) p. 235.
[21] P.A. Jacobs, J.B. Utterhoeven and H.K. Beyer, J. Chem. Soc. Faraday Trans. I 75 (1979) 56.
[22] R.G. Herman, J.H. Lunsford, H.K. Beyer, P.A. Jacobs and J.B. Utterhoeven, J. Phys. Chem. 79 (1975) 2388.
[23] P.A. Jacobs, H. Nijs and J. Verdonck, J. Chem. Soc. Faraday Trans. I 75 (1979) 1196.
[24] Y.-Y. Huang and J.R. Anderson, J. Catal. 40 (1975) 143.
[25] R.L. Garten, W.N. Delgass and M. Boudart, J. Catal. 18 (1970) 90.
[26] W.N. Delgass, R.L. Garten and M. Boudart, J. Phys. Chem. 73 (1969) 2970.
[27] K.G. Ione, L.A. Vostrikova and M.W. Mastikin, J. Mol. Catal. 31 (1985) 355.
[28] L.M. Kustov, V.B. Kazansky and P. Ratnasamy, Zeolites 7 (1987) 79.
[29] S. Kaliaguine, J.B. Nagy and Z. Gabelica, in: *Keynotes in Energy Related Catalysis*, ed. S. Kaliaguine (Elsevier, Amsterdam, 1988) p. 381.
[30] A. Raj, S. Sivasanker and K. Lázár, J. Catal. 147 (1994) 207.
[31] R. Szostak, N. Nair, D.K. Simmons, T.L. Thomas, R. Kuvadia, B. Dunson and D.C. Shieh, in: *Innovations in Zeolite Materials Science*, eds. P.J. Grobert et al. (Elsevier, Amsterdam, 1988) p. 403.
[32] P.A. Jacobs, in: *Metal Clusters in Catalysis*, eds. B.C. Gates, L. Guczi and H. Knözinger (Elsevier, Amsterdam, 1986) p. 357.
[33] E.R.S. Winter, J. Catal. 15 (1969) 144.
[34] E.R.S. Winter, J. Catal. 19 (1970) 32.
[35] G.M. Dhar and V. Srinivasan, Int. J. Chem. Kinet. 14 (1982) 415.
[36] Y.-F. Chang, J.G. McCarty and E.D. Wachsman, Appl. Catal. B, submitted.
[37] G.I. Panov, A.S. Kharitonov and V.I. Sobolev, Appl. Catal. A 98 (1993) 1.
[38] Y.-F. Chang, G.A. Somorjai and H. Heinemann, J. Catal., accepted (1994).
[39] B. Wichterlova, Zeolites 1 (1981) 181.
[40] A.V. Kucherov and A.A. Slinkin, Zeolites 6 (1986) 1754.
[41] A.V. Kucherov, A.A. Slinkin, G.K. Beyer and G. Berbely, J. Chem. Soc. Faraday Trans. I 85 (1989) 1989.